Mathematical Biosciences and Engineering

http://www.aimspress.com/journal/mbe

MBE, 20(12): 20378–20404.
DOI: 10.3934/mbe.2023901
Received: 01 August 2023
Revised: 31 October 2023
Accepted: 31 October 2023
Published: 10 November 2023

Research article

Pathogens stabilize or destabilize depending on host stage structure

Jessica L. Hite[1,*] **and André M. de Roos**[2]

[1] University of Wisconsin-Madison, Department of Pathobiological Sciences, School of Veterinary Medicine, Madison, Wisconsin, USA

[2] Institute for Biodiversity and Ecosystem Dynamics, University of Amsterdam, Amsterdam, the Netherlands; Santa Fe Institute, Santa Fe, NM 87501, USA

* **Correspondence:** Email: jhite2@wisc.edu.

Abstract: A common assumption is that pathogens more readily destabilize their host populations, leading to an elevated risk of driving both the host and pathogen to extinction. This logic underlies many strategies in conservation biology and pest and disease management. Yet, the interplay between pathogens and population stability likely varies across contexts, depending on the environment and traits of both the hosts and pathogens. This context-dependence may be particularly important in natural consumer-host populations where size- and stage-structured competition for resources strongly modulates population stability. Few studies, however, have examined how the interplay between size and stage structure and infectious disease shapes the stability of host populations. Here, we extend previously developed size-dependent theory for consumer-resource interactions to examine how pathogens influence the stability of host populations across a range of contexts. Specifically, we integrate a size- and stage-structured consumer-resource model and a standard epidemiological model of a directly transmitted pathogen. The model reveals surprisingly rich dynamics, including sustained oscillations, multiple steady states, biomass overcompensation, and hydra effects. Moreover, these results highlight how the stage structure and density of host populations interact to either enhance or constrain disease outbreaks. Our results suggest that accounting for these cross-scale and bidirectional feedbacks can provide key insight into the structuring role of pathogens in natural ecosystems while also improving our ability to understand how interventions targeting one may impact the other.

Keywords: stage-structure; eco-epidemiological feedbacks; virulence; overcompensation; bistability; hydra effect

1. Introduction

Should pathogens stabilize or destabilize their host populations? A widespread tenet is that pathogens destabilize their host populations, increasing temporal variation in density and generating larger amplitude oscillations. As populations with pronounced fluctuations are often more prone to extinction, infectious disease is generally presented as a threat to population viability and a contributing factor to species extinction [1, 2]. This prominent hypothesis is often taken at face value — notorious epidemics demonstrate the devastating effect infectious diseases can have on vulnerable species like amphibians [3, 4], Tasmanian devils [5], and American chestnuts [6]. In conservation biology, infectious disease is typically presented as a threat to population viability and a contributing factor to species extinction [1, 2].

Yet, severe and destabilizing outbreaks typically occur infrequently and in a relatively small subset of habitats [7]. For example, the virulent amphibian chytrid, *Batrachochytrium dendrobatidis* provides a recent and infamous example of how disease outbreaks can erupt catastrophically, destabilizing host populations in some contexts (e.g. permanent ponds, fragmented forests) though not others (e.g. ephemeral ponds, non-fragmented forests) [8, 9]. Why, then, does the severity and destabilizing effects of pathogens differ dramatically across habitats? If pathogens typically destabilize their host populations — increasing the risk of driving both the host and pathogen extinct — how have pathogens remained ubiquitous and widespread in ecosystems? Unfortunately, classical theory cannot answer these questions or accurately predict the impact of pathogens on population stability. This suggests that current approaches miss important biology necessary to understand how changes in pathogens will alter the functioning of natural host populations.

Part of the challenge may arise from the coarse resolution of host populations in classical epidemiological models. For complex systems like natural host-pathogen populations, a key complication lies in determining the level of detail required to improve the accuracy of predictions. Mounting evidence indicates that intraspecific variation that stems from differences in body size and developmental stage (i.e., stage structure) strongly modulates population dynamics, including the density, demographic structure, and stability of consumer-resource systems. For instance, accounting for differences in how individuals transition through various life stages and compete for resources helps explain puzzling patterns seen in empirical studies including oscillatory dynamics, bistability, biomass overcompensation, and hydra effects [10, 11]. "Biomass overcompensation" occurs when the biomass density, often of a particular size or stage class, increases in response to elevated mortality [12]. Similarly, "hydra effects" can occur when higher mortality reduces the amplitude of population cycles, when mortality precedes overcompensatory density dependence, or decreases consumption rates leading to increased resource productivity and thus, population density [13].

Given such pronounced effects on the demography and density of host populations, stage-structured interactions among hosts should strongly impact disease dynamics, and vice versa. Despite the potentially far-reaching consequences of stage structure on both food webs and epidemiological dynamics, these interactions have traditionally been overlooked in classical theory [14–16]). Epidemiological theory in particular has traditionally made a number of simplifying assumptions that omit important components of stage structure in host populations.

First, models typically assume that host populations are homogeneous. That is, all hosts are equally affected by infection and carry the same value for the pathogen. Juvenile and adult hosts, however,

differ in quality because of natural variation in host resistance, medical treatments, or sex-based differences in immunity. Age, in particular, is well-known to influence the manifestation and pathophysiology of disease in plants [17, 18], wildlife [15, 19], and humans [20, 21]. Such differences carry important epidemiological (and evolutionary) consequences. In other words, the pathogen now faces the challenge of exploiting a heterogeneous host population, and the structure (frequency and density) of each host type governs the fitness of the pathogen [22–24].

Second, virulence (infection-mediated harm caused to hosts) is most often defined as an increase in mortality [25, 26]. Although the focus on mortality has enabled easy comparisons among models and certainly helped to advance the field, this simplification overlooks other critical aspects of infection. For example, virulence often involves sublethal effects (morbidity) that divert energy away from essential physiological needs and costly immune functions towards pathogen growth. Such increases in basic maintenance costs can reduce the energy available to support development and reproduction. Fecundity, in particular, can be reduced to the point of sterilization, as seen in numerous vertebrate and invertebrate hosts. Changes in these life history traits will differ across juvenile and adult hosts and carry pronounced consequences for both the stability and structure of host populations in ways that can feedback to influence epidemiological dynamics [27–29].

Moreover, variation in virulence and the stage structure of host populations are ubiquitous in natural host-pathogen systems [15, 19] and are often mechanistically linked via resources through numerous pathways [18, 30, 31]. For example, juveniles and adults often compete for resources, and different environmental conditions can cause a change in which stage is competitively superior and controls the resource [12]. Resources also govern the energy available to hosts to support immune responses (and other traits of life history) and, therefore, may influence various forms of lethal and sublethal virulence [26,27,29]. Our understanding of the interplay between these ecological and epidemiological factors remains fragmentary.

The physiologically-structured framework [12] developed here is well suited to examine both lethal and sublethal (energetic) forms of virulence in size/stage-structured host populations for at least three key reasons. First, this approach mechanistically links individual and population-level processes because it adheres to a strict mass-conservation principle. This important detail accounts for processes by which energy is acquired (feeding) and through which energy is spent (maintenance, growth, reproduction, and immunity). More specifically, the consumer-host has a simplified asexual life history in which a) food intake and metabolic demands scale linearly with body size; b) the rate at which individuals grow and develop depends on food density; and c) juvenile individuals allocate all of their energy into somatic growth, whereas adult individuals allocate all of their energy to reproduction. Second, unlike previous models for stage-structured disease, this framework captures the resource-dependent dynamics of juvenile hosts across a continuous size distribution. Finally, the initial demographic structure of the susceptible host population is determined by changes in the stage-specific competitive ability of juvenile and adult hosts.

2. Materials and methods

2.1. Model formulation

We base our model on a size-structured consumer-resource model presented in de Roos, Metz and Persson [10] (Eqs. (39) therein; see also Box 9.1 in [12]), but adapt our notation to account for suscep-

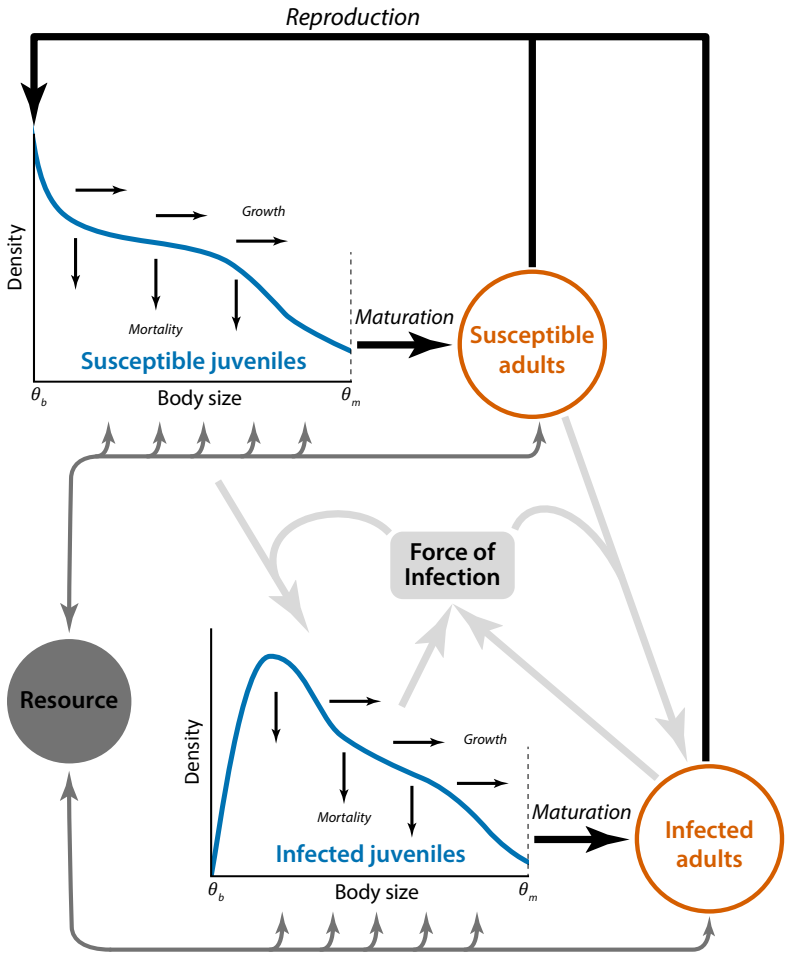

Figure 1. Schematic overview of the size-structured consumer-resource model with SI infection dynamics. Susceptible and infected juveniles are represented by their size-distribution, whereas susceptible and infected adults are represented by their numerical densities. Black arrows represent life history processes. Dark-gray arrows represent consumer-resource interactions (feeding, food-dependent growth, mortality and reproduction). Light-gray arrows represent infection dynamics. Infected juveniles and adults contribute equally to the force of infection.

tible and infected individuals (See Figure 1 for a schematic overview of the model and its components). In the model individuals are characterized by their body size (i.e. mass) θ, having a size at birth equal to θ_b and maturing on reaching a maturation size threshold $\theta = \theta_m$. All individuals feed on a shared resource R following a type II functional response, $R/(H + R)$, in which H is the half-saturation resource density. In the absence of consumers the resource follows semi-chemostat dynamics (see Persson et al. [32] for explanation and justification). Food intake, maintenance costs, growth in body size, and reproduction are all assumed to be proportional to individual body size θ. To phenomenologically capture differences in the food limitation of juveniles and adults, we assume that their maximum mass-specific feeding rate is equal to $(2 - q)M$ and qM, respectively, where the parameter M represents a scaling constant for the maximum ingestion rate. The parameter q represents stage-specific competitive ability,

which mechanistically, translates to asymmetries in feeding rates. With $q > 1$, juvenile development (growth in body size) is more food-limited than adult reproduction and $q < 1$ implies the opposite [10]. Food ingestion by juvenile and adult individuals hence equals

$$\omega_J(R)\theta = (2-q)\, M\frac{R}{H+R}\theta \tag{2.1}$$

and

$$\omega_A(R)\theta_m = qM\frac{R}{H+R}\theta_m \tag{2.2}$$

respectively. We assume that ingested food is assimilated with a constant efficiency σ that includes all overhead costs associated with growth in body size or production of offspring. We assume a net production model for individual energetics [33], so that the assimilated food is first used to cover maintenance costs. Assuming that the mass-specific maintenance requirements, indicated by T, are the same for juveniles and adults, the net-energy production that remains after covering maintenance costs equals

$$\nu_{S_J}(R)\theta = (\sigma\omega_J(R) - T)\,\theta \tag{2.3}$$

for juveniles and

$$\nu_{S_A}(R)\theta_m = (\sigma\omega_A(R) - T)\,\theta_m \tag{2.4}$$

for adults. Juvenile consumer-hosts invest their net energy into somatic growth, while adults invest it all in reproduction, and hence do not grow. Growth and reproduction stop, however, whenever resource densities are so low that either $\nu_{S_J}(R)$ or $\nu_{S_A}(R)$ are negative. We introduce the shorthand notation $f^+(R)$ and $f^-(R)$ to indicate the value of the function $f(R)$ restricted to non-negative and non-positive values, respectively, i.e. $f^+(R) = \max(f(R), 0)$ and $f^-(R) = \min(f(R), 0)$. If net-energy production is negative, juvenile and adult individuals are assumed to experience an increased mortality rate equal to

$$d_{S_J}(R) = \mu_S - \nu^-_{S_J}(R) \tag{2.5}$$

and

$$d_{S_A}(R) = \mu_S - \nu^-_{S_A}(R) \tag{2.6}$$

respectively [34], where μ_S indicates the background mortality rate of susceptible individuals.

In the absence of disease, the size-structured consumer-resource model can now be expressed in terms of a partial differential equation (PDE) for the juvenile size-distribution $s_J(t,\theta)$ and ordinary differential equations (ODEs) for the number of adult individuals $S_A(t)$ and the resource density R:

$$\frac{dR}{dt} = \rho\,(R_{max} - R) - \omega_J(R)\int_{\theta_b}^{\theta_m}\theta s_J(t,\theta)d\theta \;-\; \omega_A(R)\theta_m S_A \tag{2.7}$$

$$\frac{\partial s_J(t,\theta)}{\partial t} + \frac{\partial(\nu^+_{S_J}(R)\theta s_J(t,\theta))}{\partial\theta} = -d_{S_J}(R)s_J(t,\theta) \tag{2.8}$$

$$\nu^+_{S_J}(R)\theta_b s_J(t,\theta_b) = \frac{\nu^+_{S_A}(R)\theta_m S_A}{\theta_b} \tag{2.9}$$

$$\frac{dS_A}{dt} = \nu^+_{S_J}(R)\theta_m s_J(t,\theta_m) - d_{S_A}(R)S_A \tag{2.10}$$

To account for the spread of a pathogen in this size-structured model of susceptible consumer-hosts feeding on a shared resource, we extend the model with a size-distribution $i_J(t,\theta)$ of infected juvenile consumer-hosts and a density $I_A(t)$ of infected adult consumer-hosts. We assume the force of infection $\lambda(t)$ to be proportional to the total number of infected individuals with proportionality constant β:

$$\lambda(t) = \beta\left(\int_{\theta_b}^{\theta_m} i_J(t,\theta)\,d\theta + I_A(t)\right) \tag{2.11}$$

We then examine the epidemiological and population dynamic consequences of pathogens that either increase basic maintenance costs or increase mortality rates. More specifically, virulence can either increase mass-specific maintenance requirements from T to $(1+c_T)T$ or increase in the mortality rate from μ_S to

$$\mu_I = (1+c_\mu)\mu_S \tag{2.12}$$

in which c_T and c_μ represent, in a relative sense the negative consequences of being infected (virulence). If infected individuals experience increased maintenance requirements, their growth rate in body size as a juvenile and reproduction rate as adults will be reduced and given by:

$$\nu_{I_J}(R)\theta = (\sigma\omega_J(R) - (1+c_T)\,T)\,\theta \tag{2.13}$$

for juveniles and

$$\nu_{I_A}(R)\theta_m = (\sigma\omega_A(R) - (1+c_T)\,T)\,\theta_m \tag{2.14}$$

for adults. Note, however, that for simplicity, we assume that infected individuals do not reduce their feeding rates, which is part of the innate immune response and common in many host-pathogen systems [35]. We will consider only horizontal transmission of the disease without any recovery. The size-structured consumer-resource model with SI infection dynamics can then be summarized with the following system of PDEs and ODEs:

$$\frac{dR}{dt} = \rho\,(R_{max} - R) - \omega_J(R)\int_{\theta_b}^{\theta_m}\theta\,(s_J(t,\theta) + i_J(t,\theta))\,d\theta \;-\; \omega_A(R)\theta_m\,(S_A + I_A) \tag{2.15}$$

$$\frac{\partial s_J(t,\theta)}{\partial t} + \frac{\partial(\nu^+_{S_J}(R)\theta s_J(t,\theta))}{\partial\theta} = -\left(d_{S_J}(R) + \lambda(t)\right)s_J(t,\theta) \tag{2.16}$$

$$\nu^+_{S_J}(R)\theta_b s_J(t,\theta_b) = \frac{\nu^+_{S_A}(R)\theta_m S_A + \nu^+_{I_A}(R)\theta_m I_A}{\theta_b} \tag{2.17}$$

$$\frac{dS_A}{dt} = \nu^+_{S_J}(R)\theta_m s_J(t,\theta_m) - \left(d_{S_A}(R) + \lambda(t)\right)S_A \tag{2.18}$$

$$\frac{\partial i_J(t,\theta)}{\partial t} + \frac{\partial(\nu^+_{I_J}(R)\theta i_J(t,\theta))}{\partial\theta} = -d_{I_J}(R)i_J(t,\theta) + \lambda(t)s_J(t,\theta) \tag{2.19}$$

$$\nu^+_{I_J}(R)\theta_b i_J(t,\theta_b) = 0 \tag{2.20}$$

$$\frac{dI_A}{dt} = \nu^+_{I_J}(R)\theta_m i_J(t,\theta_m) - d_{I_A}(R)I_A + \lambda(t)S_A \tag{2.21}$$

Table 1. Parameters and default values for the size-structured consumer-resource model with SI infection dynamics [10].

Parameter	Description	Default value
ρ	Resource turnover rate	0.1
R_{max}	Resource maximum biomass density	100
θ_b	Size at birth	0.1
θ_m	Size at maturation	1.0
M	Mass-specific maximum ingestion rate scalar	1.0
q	Juvenile-adult ingestion rate asymmetry	0.75 or 1.25
H	Half saturation resource density	3.0
T	Mass-specific maintenance rate	0.1
σ	Conversion efficiency	0.5
μ_S	Background mortality rate	0.015
β	Force of infection scaling constant	$1.0 \cdot 10^{-3}$
c_T	Relative increase in maintenance costs due to infection	1.0
c_μ	Relative increase in background mortality due to infection	5.0

$$\lambda(t) = \beta\left(\int_{\theta_b}^{\theta_m} i_J(t,\theta)d\theta + I_A(t)\right) \tag{2.22}$$

in which the functions $d_{I_J}(R)$ and $d_{I_A}(R)$ indicate the death rate of infected juvenile and adult individuals, respectively, defined as:

$$d_{I_J}(R) = \mu_I - \nu^-_{I_J}(R) \tag{2.23}$$

and

$$d_{I_A}(R) = \mu_I - \nu^-_{I_A}(R) \tag{2.24}$$

Parameters of the model and their default values are presented in Table 1.

2.2. Disease free equilibrium

The equilibrium state of the uninfected consumer-host population is determined by the equilibrium density of the resource $\tilde{R}$ and the equilibrium birth rate $\tilde{b}$ of the consumer-host, which can be calculated following the procedures in Diekmann, Metz and Gyllenberg [36]. (Here and below we use tildes to indicate the equilibrium value of a particular variable). Notice that in an equilibrium situation starvation mortality does not occur, hence $\nu^-_{S_J}(R) = \nu^-_{S_A}(R) = 0$, $\nu^+_{S_J}(R) = \nu_{S_J}(R) > 0$ and $\nu^+_{S_A}(R) = \nu_{S_A}(R) > 0$. Furthermore, to simplify the notation we drop the function argument R of ν_{S_J} and ν_{S_A} and we introduce the parameter z to indicate the ratio of the size at birth and maturation, $z = \theta_b/\theta_m$.

In the pathogen-free equilibrium, juveniles grow at a mass-specific rate equal to ν_{S_J} with mortality

rates equal to μ_S. Growth in body size hence follows:

$$\theta(a) \;=\; \theta_b \exp(\nu_{S_J} a) \tag{2.25}$$

which implies that individuals mature at an age

$$a_m \;=\; -\frac{\ln z}{\nu_{S_J}} \tag{2.26}$$

Given that individual survival is given by $F(a) = \exp(-\mu_S a)$ the probability to survive up to maturation equals

$$F_{m_S} \;=\; z^{\frac{\mu_S}{\nu_{S_J}}}$$

After maturation, an individual has an expected lifetime equal to $1/\mu_S$ and reproduces at a rate ν_{S_A}/z. The expected lifetime reproductive output at a constant resource density $\tilde{R}$ therefore equals:

$$L \;=\; \frac{\nu_{S_A}}{\mu_S} z^{\frac{\mu_S}{\nu_{S_J}}-1} \tag{2.27}$$

Substituting parameter values and solving $L = 1$ yields the value of the equilibrium resource density ($\tilde{R} = 0.8961$ for default parameter values).

In equilibrium, the integral term in the right-hand side of ODE (2.7), which represents resource ingestion by juveniles, can be evaluated by reformulating it as an integral over the age interval from 0 till a_m and using the population age distribution, which is given by $\tilde{b}\exp(-\mu_S a)$:

$$\omega_J(\tilde{R}) \int_{\theta_b}^{\theta_m} \theta \tilde{s}_J(\theta) d\theta = \omega_J(\tilde{R}) \int_0^{a_m} \theta_b e^{\nu_{S_J} a}\, \tilde{b} e^{-\mu_S a} da = \omega_J(\tilde{R})\, \tilde{b}\, \frac{\theta_m z^{\frac{\mu_S}{\nu_{S_J}}} - \theta_b}{\nu_{S_J} - \mu_S}$$

The value of the adult consumer-host density in equilibrium can be calculated by equating the right-hand side of the ODE (2.10) to 0 and by using the fact that in equilibrium the rate of maturation $\nu_{S_J}\theta_m \tilde{s}_J(\theta_m)$ equals the product of the total population birth rate and the survival probability till maturation $\tilde{b}F_{m_S}$:

$$\tilde{S}_A = \frac{\nu_{S_J}\theta_m \tilde{s}_J(\theta_m)}{\mu_S} = \tilde{b}\, \frac{z^{\frac{\mu_S}{\nu_{S_J}}}}{\mu_S}$$

The last term in the right-hand side of ODE (2.7), which represents resource ingestion by adults, can hence be expressed as:

$$\omega_A(\tilde{R})\, \theta_m\, \tilde{S}_A = \omega_A(\tilde{R})\, \theta_m\, \tilde{b}\, \frac{z^{\frac{\mu_S}{\nu_{S_J}}}}{\mu_S}$$

The equilibrium birth rate $\tilde{b}$ can then be computed by substituting these expressions into the right-hand side of the ODE (2.7) and equating it to 0:

$$\tilde{b} = \frac{\rho\left(R_{max} - \tilde{R}\right)}{\omega_J(\tilde{R})\, \dfrac{\theta_m z^{\frac{\mu_S}{\nu_{S_J}}} - \theta_b}{\nu_{S_J} - \mu_S} + \omega_A(\tilde{R})\, \dfrac{\theta_m z^{\frac{\mu_S}{\nu_{S_J}}}}{\mu_S}} \tag{2.28}$$

Notice that this is an explicit expression for $\tilde{b}$, provided that $\tilde{R}$ is known.

2.3. Calculation of R_0

The basic reproductive number R_0 is defined as the number of secondary infections caused by a single infected individual [37]. For a pathogen to successfully invade the host population $R_0 > 1$, whereas when $R_0 < 1$ the epidemic dies out. Because in the structured model individuals can be infected at different body sizes (or equivalently, different ages), we calculate R_0 following Heesterbeek and Dietz [38], who show that under scenarios where all uninfected individuals are equally susceptible to the disease, independent of their age or body size, the value of R_0 can be calculated as:

$$R_0 = \int_0^\infty k(\eta)\, G(\eta)\, d\eta$$

in which the function $k(\eta)$ represents the lifetime contribution of an individual that is infected at age η towards the force of infection and $G(\eta)$ is the stable age distribution in the pathogen-free equilibrium population.

Since juvenile and adult individuals are modeled separately, the expression for R_0 in our model for a pathogen invading a fully susceptible consumer-host population in equilibrium with its resource can be written as:

$$\begin{aligned} R_0 &= \int_0^{a_m} k(\eta)\, \tilde{b} \exp(-\mu_S \eta)\, d\eta + k(a_m)\tilde{S}_A \\ &= \int_0^{a_m} k(\eta)\, \tilde{b} \exp(-\mu_S \eta)\, d\eta + k(a_m)\, \tilde{b}\, \frac{z^{\frac{\mu_S}{\nu_{S_J}}}}{\mu_S} \end{aligned} \tag{2.29}$$

in which we have also substituted the expression for the stable age distribution, $G(a) = \tilde{b} \exp(-\mu_S a)$. The contribution $k(a_m)$ to the force of infection by an individual that is infected in the adult stage equals the product of β and the expected lifetime of an individual:

$$k(a_m) = \frac{\beta}{d_{I_A}} \tag{2.30}$$

Notice that in this and the following sections, we will consistently omit the function argument R of functions like $d_{I_A}(R)$. If a juvenile individual becomes infected at age η it has a body mass $\theta_b \exp(\nu_{S_J}\eta)$. After infection the individual will grow at a mass-specific rate $\nu^+_{I_J}$ and therefore follow a growth curve given by:

$$\theta_{I_J}(a,\eta) \;=\; \theta_b\, e^{\nu_{S_J}\eta}\, e^{\nu^+_{I_J}(a-\eta)} \;=\; \theta_b\, e^{(\nu_{S_J} - \nu^+_{I_J})\eta}\, e^{\nu^+_{I_J} a}$$

reaching maturation at age

$$a_{m_I}(\eta) \;=\; \frac{-\ln z - (\nu_{S_J} - \nu^+_{I_J})\eta}{\nu^+_{I_J}}$$

Since the survival function following infection is given by $\exp\left(-d_{I_J}\,(a-\eta)\right)$ $(a > \eta)$, the probability of a juvenile surviving to maturation following infection at age η equals:

$$F_{m_I}(\eta) \;=\; \exp\left(-d_{I_J}\left(\frac{-\ln z - (\nu_{S_J} - \nu^+_{I_J})\eta}{\nu^+_{I_J}} - \eta\right)\right) \;=\; z^{\frac{d_{I_J}}{\nu^+_{I_J}}}\, e^{\nu_{S_J}\frac{d_{I_J}}{\nu^+_{I_J}}\eta} \tag{2.31}$$

The contribution of this individual to the force of infection during the juvenile stage is then given by:

$$\beta \int_{\eta}^{a_{m_I}(\eta)} \exp\left(-d_{I_J}\left(a-\eta\right)\right) da = \frac{\beta}{d_{I_J}} - \frac{\beta F_{m_I}(\eta)}{d_{I_J}}$$

while the contribution to the force of infection as an adult is the same as the expected contribution of an individual that is infected as an adult. For individuals that become infected as a juvenile ($a < a_m$) the function $k(\eta)$ is hence given by:

$$\begin{aligned} k(\eta) &= \frac{\beta}{d_{I_J}} + \left(\frac{\beta}{d_{I_A}} - \frac{\beta}{d_{I_J}}\right) F_{m_I}(\eta) \\ &= \frac{\beta}{d_{I_J}} + \left(\frac{\beta}{d_{I_A}} - \frac{\beta}{d_{I_J}}\right) z^{\frac{d_{I_J}}{\nu^+_{I_J}}} e^{\nu_{S_J}\frac{d_{I_J}}{\nu^+_{I_J}}\eta} \end{aligned} \tag{2.32}$$

It should be noted, however, that the second term in this expression equals 0 in cases where infected juvenile individuals are starving ($\nu_{I_J} < 0$) because in that case $\nu^+_{I_J} = 0$ and hence $F_{m_I}(\eta) = 0$.

Substitution of the expressions for $k(\eta)$ (eq. (2.32)) and $k(a_m)$ (eq. (2.30)) into equation (2.29) for R_0 then yields:

$$R_0 = \beta\,\tilde{b}\left(\frac{1 - z^{\frac{\mu_S}{\nu_{S_J}}}}{\mu_S d_{I_J}} + \frac{z^{\frac{\mu_S}{\nu_{S_J}}}}{\mu_S d_{I_A}} + \nu^+_{I_J}\left(\frac{1}{d_{I_A}} - \frac{1}{d_{I_J}}\right)\frac{z^{\frac{\mu_S}{\nu_{S_J}}} - z^{\frac{d_{I_J}}{\nu^+_{I_J}}}}{\nu_{S_J} d_{I_J} - \mu_S \nu^+_{I_J}}\right) \tag{2.33}$$

2.4. Equilibrium state with the pathogen

The equilibrium state of the model with infected individuals is uniquely determined by three unknown quantities: the resource density in equilibrium, $\tilde{R}$, the population birth rate in equilibrium, $\tilde{b}$, and the force of infection in equilibrium, $\tilde{\lambda}$. All other population-level quantities can be expressed in terms of these three variables. In the following, we derive conditions that determine the value of these three variables in an equilibrium state. Notice that in an equilibrium situation, starvation mortality does not occur for susceptible individuals, hence $\nu^-_{S_J}(R) = \nu^-_{S_A}(R) = 0$, $\nu^+_{S_J}(R) = \nu_{S_J}(R) > 0$ and $\nu^+_{S_A}(R) = \nu_{S_A}(R) > 0$. In contrast, infected juveniles and adults could still starve, so ν_{I_J} and ν_{I_A} could in principle be negative. As before, we simplify notation by dropping the function argument R to all resource-dependent functions, such as ν_{S_J}, ν_{S_A}, ν_{I_J} and ν_{I_A}, and use the parameter z to indicate the ratio of the size at birth and maturation, $z = \theta_b/\theta_m$.

The density of susceptible, newborn individuals in equilibrium can be written as:

$$\tilde{s}_J(\theta_b) = \frac{\tilde{b}}{\nu_{S_J}\,\theta_b}$$

where $\tilde{b}$ represents the population birth rate in equilibrium. The equilibrium density of susceptible juveniles changes with size following the ODE:

$$\frac{d}{d\theta}\left(\nu_{S_J}\theta\tilde{s}_J(\theta)\right) = -\left(\mu_S + \tilde{\lambda}\right)\tilde{s}_J(\theta)$$

which can be solved to

$$\tilde{s}_J(\theta) \;=\; \frac{\tilde{b}}{\nu_{S_J}\,\theta_b}\left(\frac{\theta_b}{\theta}\right)^{1+x}$$

in which x is introduced to denote

$$x = \frac{\mu_S + \tilde{\lambda}}{\nu_{S_J}} \tag{2.34}$$

The total number of susceptible juvenile individuals in equilibrium, which we denote by $\tilde{S}_J$, then equals:

$$\tilde{S}_J \;=\; \int_{\theta_b}^{\theta_m} \frac{\tilde{b}}{\nu_{S_J}\,\theta_b}\left(\frac{\theta_b}{\theta}\right)^{1+x} d\theta \;=\; \frac{\tilde{b}}{\nu_{S_J}}\frac{(1-z^x)}{x} \tag{2.35}$$

Let $\tilde{B}_{S_J}$ denote the total biomass of susceptible juvenile individuals in equilibrium, which equals the integral of $\theta\tilde{s}_J(\theta)$ from θ_b to θ_m:

$$\tilde{B}_{S_J} \;=\; \int_{\theta_b}^{\theta_m} \theta\frac{\tilde{b}}{\nu_{S_J}\,\theta_b}\left(\frac{\theta_b}{\theta}\right)^{1+x} d\theta \;=\; \frac{\tilde{b}\,\theta_b}{\nu_{S_J}}\frac{\left(1-z^{x-1}\right)}{x-1} \tag{2.36}$$

The maturation rate of susceptible juveniles equals

$$\nu_{S_J}\theta_m\tilde{s}_J(\theta_m) \;=\; \tilde{b}\,z^x$$

such that the numerical density of susceptible adult individuals in equilibrium is given by:

$$\tilde{S}_A \;=\; \frac{\tilde{b}}{\mu_S + \tilde{\lambda}}z^x \tag{2.37}$$

while the total biomass of susceptible adult individuals in equilibrium, indicated with $\tilde{B}_{S_A}$, is given by:

$$\tilde{B}_{S_A} \;=\; \frac{\tilde{b}\,\theta_m}{\mu_S + \tilde{\lambda}}z^x \tag{2.38}$$

The equilibrium density of infected juveniles changes with size following the ODE:

$$\frac{d}{d\theta}\left(\nu_{I_J}^+\theta\tilde{i}_J(\theta)\right) = \; -d_{I_J}\tilde{i}_J(\theta) + \tilde{\lambda}\tilde{s}_J(\theta)$$

Using the explicit expression for $\tilde{s}_J(\theta)$, together with its boundary condition $\tilde{i}_J(\theta_b) = 0$, can be solved to yield:

$$\tilde{i}_J(\theta) = \frac{\tilde{b}}{\nu_{S_J}\theta}\frac{\tilde{\lambda}}{d_{I_J} - \nu_{I_J}^+ x}\left(\left(\frac{\theta_b}{\theta}\right)^x - \left(\frac{\theta_b}{\theta}\right)^{\frac{d_{I_J}}{\nu_{I_J}^+}}\right)$$

which can be rewritten as:

$$\tilde{i}_J(\theta) = \frac{\tilde{\lambda}}{d_{I_J} - \nu_{I_J}^+ x}\left(1 - \left(\frac{\theta_b}{\theta}\right)^{\frac{d_{I_J}}{\nu_{I_J}^+} - x}\right)\tilde{s}_J(\theta)$$

The total number of infected juvenile individuals in equilibrium, $\tilde{I}_J$, which equals the integral of $\tilde{i}_J(\theta)$ from $\theta_b = z\theta_m$ to θ_m, can be evaluated to:

$$\tilde{I}_J = \frac{\tilde{b}}{\nu_{S_J}} \frac{\tilde{\lambda}}{d_{I_J} x} \left(1 + \frac{\nu_{I_J}^+ x \, z^{\frac{d_{I_J}}{\nu_{I_J}^+}}}{d_{I_J} - \nu_{I_J}^+ x} - \frac{d_{I_J} z^x}{d_{I_J} - \nu_{I_J}^+ x} \right)$$

This expression can be rewritten in a more compact form as:

$$\tilde{I}_J = \frac{\tilde{\lambda}}{d_{I_J}} \left(\tilde{S}_J + \nu_{I_J}^+ \frac{\tilde{b}}{\nu_{S_J}} \frac{z^{\frac{d_{I_J}}{\nu_{I_J}^+}} - z^x}{d_{I_J} - \nu_{I_J}^+ x} \right) \tag{2.39}$$

Let $\tilde{B}_{I_J}$ denote the total biomass of infected juvenile individuals in equilibrium, which equals the integral of $\theta \tilde{i}_J(\theta)$ from θ_b to θ_m:

$$\tilde{B}_{I_J} = \int_{\theta_b}^{\theta_m} \theta \frac{\tilde{\lambda}}{d_{I_J} - \nu_{I_J}^+ x} \left(1 - \left(\frac{\theta_b}{\theta} \right)^{\frac{d_{I_J}}{\nu_{I_J}^+} - x} \right) \tilde{s}_J(\theta) \, d\theta$$

This integral can be evaluated and expressed in terms of $\tilde{B}_{S_J}$, yielding:

$$\tilde{B}_{I_J} = \frac{\tilde{\lambda}}{d_{I_J} - \nu_{I_J}^+ x} \left(\tilde{B}_{S_J} - \nu_{I_J}^+ \frac{\tilde{b}\,\theta_b}{\nu_{S_J}} \frac{1 - z^{\frac{d_{I_J}}{\nu_{I_J}^+} - 1}}{d_{I_J} - \nu_{I_J}^+} \right) \tag{2.40}$$

Notice that in cases where infection causes juvenile individuals to have such high maintenance costs that they are starving, implying that $\nu_{I_J}^+ = 0$, the second term within parentheses in expression (2.39) and in (2.40) vanishes.

The maturation rate of infected juveniles equals:

$$\nu_{I_J}^+ \theta_m \tilde{i}_J(\theta_m) = \nu_{I_J}^+ \frac{\tilde{\lambda}}{d_{I_J} - \nu_{I_J}^+ x} \left(1 - z^{\frac{d_{I_J}}{\nu_{I_J}^+} - x} \right) \theta_m \tilde{s}_J(\theta_m) = \nu_{I_J}^+ \frac{\tilde{\lambda}}{d_{I_J} - \nu_{I_J}^+ x} \left(1 - z^{\frac{d_{I_J}}{\nu_{I_J}^+} - x} \right) \frac{\mu_S + \tilde{\lambda}}{\nu_{S_J}} \tilde{S}_A$$

Equating the right-hand side of the ODE (2.21) to 0 and substituting this expression for the maturation rate of infected juveniles allows for deriving the following relationship between the total density of infected adults, indicated with $\tilde{I}_A$, and the total density of susceptible adults $\tilde{S}_A$:

$$\tilde{I}_A = \frac{\tilde{\lambda}}{d_{I_A}} \left(1 + \frac{\nu_{I_J}^+}{d_{I_J} - \nu_{I_J}^+ x} \left(1 - z^{\frac{d_{I_J}}{\nu_{I_J}^+} - x} \right) \frac{\mu_S + \tilde{\lambda}}{\nu_{S_J}} \right) \tilde{S}_A \tag{2.41}$$

Correspondingly, the total biomass of infected adults, $\tilde{B}_{I_A}$, is given by:

$$\tilde{B}_{I_A} = \frac{\tilde{\lambda}}{d_{I_A}} \left(1 + \frac{\nu_{I_J}^+}{d_{I_J} - \nu_{I_J}^+ x} \left(1 - z^{\frac{d_{I_J}}{\nu_{I_J}^+} - x} \right) \frac{\mu_S + \tilde{\lambda}}{\nu_{S_J}} \right) \tilde{B}_{S_A} \tag{2.42}$$

Using the expressions derived above for the density and biomass of susceptible juveniles and adults, we can now write down the three conditions that determine the equilibrium state of the model with infections. The first condition ensures that the population birth rate $\tilde{b}$ equals the total reproduction rate of the population. Per-capita fecundity of susceptible and infected adults is equal to $\nu_{S_A}\,\theta_m/\theta_b$ and $\nu^+_{I_A}\,\theta_m/\theta_b$, respectively. The total population birth rate is hence equal to

$$\tilde{b} = \frac{\nu_{S_A}\,\tilde{B}_{S_A} \,+\, \nu^+_{I_A}\,\tilde{B}_{I_A}}{\theta_b}$$

which can be rewritten as:

$$\frac{z^{x-1}}{\mu_S + \tilde{\lambda}}\left(\nu_{S_A} + \nu^+_{I_A}\,\frac{\tilde{\lambda}}{d_{I_A}}\left(1 + \frac{\nu^+_{I_J}}{d_{I_J} - \nu^+_{I_J}x}\left(1 - z^{\frac{d_{I_J}}{\nu^+_{I_J}}-x}\right)\frac{\mu_S + \tilde{\lambda}}{\nu_{S_J}}\right)\right) \;=\; 1 \tag{2.43}$$

This condition contains as unknowns the force of infection $\tilde{\lambda}$ in equilibrium and the equilibrium resource density $\tilde{R}$, which influences ν_{S_J}, $\nu^+_{I_J}$, ν_{S_A}, $\nu^+_{I_A}$, d_{I_J} and d_{I_A}.

Next, in equilibrium the turnover rate of resource $\rho\left(R_{max} - \tilde{R}\right)$ has to equal the total foraging rate of the population. This equilibrium condition is hence given by:

$$\rho\left(R_{max} - \tilde{R}\right) \;=\; \omega_J(\tilde{R})\,\left(\tilde{B}_{S_J} + \tilde{B}_{I_J}\right) \,+\, \omega_A(\tilde{R})\,\left(\tilde{B}_{S_A} + \tilde{B}_{I_A}\right) \tag{2.44}$$

with the quantities $\tilde{B}_{S_J}$, $\tilde{B}_{I_J}$, $\tilde{B}_{S_A}$ and $\tilde{B}_{I_A}$ given by equations (2.36), (2.40), (2.38) and (2.42), respectively. This condition contains all equilibrium variables $\tilde{R}$, $\tilde{b}$ and λ as unknowns. The last identity relates the force of infection in equilibrium $\tilde{\lambda}$ to the total numerical density of infected juvenile and adult individuals:

$$\tilde{\lambda} \;=\; \beta\left(\tilde{I}_J \,+\, \tilde{I}_A\right) \tag{2.45}$$

Equilibrium states of the model can now be computed by numerically solving the equations (2.43), (2.44) and (2.45) for the unknowns $\tilde{R}$, $\tilde{b}$ and $\tilde{\lambda}$.

2.5. Computations of population dynamics

In addition to computations of the equilibrium states of the model as a function of asymmetries in stage-specific competitive ability (juvenile-adult ingestion rate, q) and as a function of the force of infection (scaling constant, β), we used numerical integration to analyze the model. Numerical integration was performed using the Escalator Boxcar Train method that is specifically developed to study the dynamics of physiologically structured populations [39, 40]. The results of the numerical integration confirmed the results from the equilibrium computations under stable steady-state conditions. In addition, numerical integration revealed the occurrence of limit cycles in population densities whenever the steady state was destabilized through a Hopf bifurcation.

3. Results

3.1. Effect of host population structure on pathogen invasion

Figure 2 shows the equilibrium densities of the susceptible population in the absence of pathogens as a function of stage-specific competitive ability (the asymmetry in juvenile-adult ingestion rate parameter, q). For low values of q, juveniles are competitively superior, adults have lower mass-specific

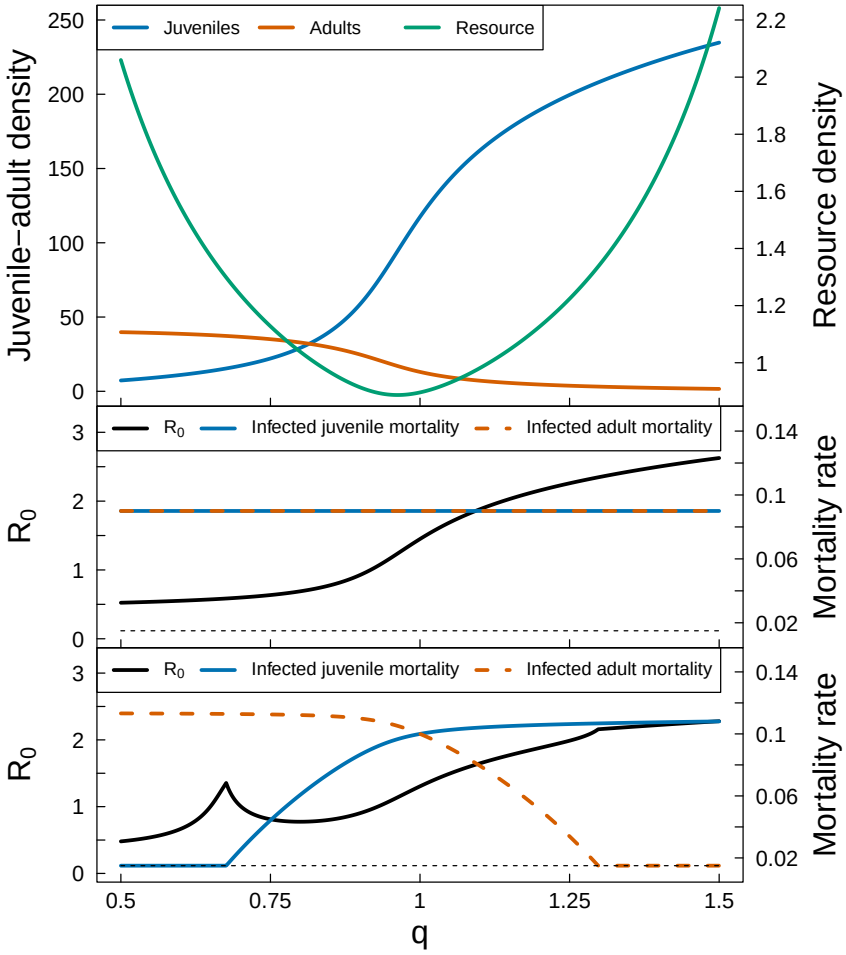

Figure 2. *Top*: Equilibrium densities of resources (green), juvenile (blue), and adult (orange) consumer-hosts in the pathogen-free steady state as a function of stage-specific competitive ability (the asymmetry in juvenile-adult ingestion rate parameter, q). *Middle*: Pathogen fitness, R_0 (black), infected juvenile (blue), and adult (orange) mortality rates as a function of stage-specific competitive ability (q) when virulence increases mortality rates (infected individuals experience an increase in mortality rate that is six times the mortality rate of susceptible individuals, $c_\mu = 5.0$). *Bottom*: Pathogen fitness R_0 (black), infected juvenile (blue), and adult (orange) mortality rates as a function of stage-specific competitive ability (q) increases maintenance costs (infected individuals have double the maintenance costs of susceptible individuals, $c_T = 1.0$). See Table 1 for parameter values.

ingestion rates relative to juveniles and hence reproduction is more food-limited than maturation. This leads to rapid juvenile development and a bottleneck in the adult stage. As a consequence, the density of juveniles is low and the population is dominated by adults. With increasing values of q, adults gain more of a competitive advantage (adults have higher mass-specific ingestion rates relative to juveniles), and maturation becomes more food-limited. These changes lead to delayed juvenile development and the density of susceptible juveniles increases, while adult density decreases [12]. The equilibrium resource density remains high for both low and high values of q, reaching a minimum at a value of q just

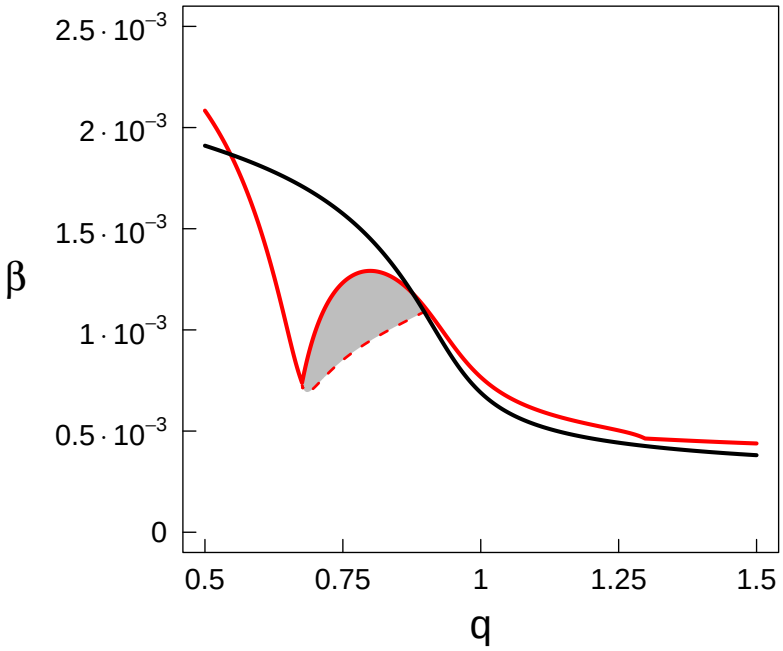

Figure 3. The force of infection scaling constant (β), that allows for pathogen invasion across a gradient in host demographics where populations transition from adult-dominated ($q < 1$) to juvenile dominated ($q > 1$), where q is the ingestion rate parameter that governs stage-specific competitive ability. This minimum value of β allowing for pathogen invasion depends on host population structure and whether virulence increases mortality rates (six times that of susceptible individuals, $c_\mu = 5.0$; black solid curve) or when virulence increases maintenance costs (double the maintenance costs of susceptible individuals, $c_T = 1.0$; red solid curve). When virulence increases maintenance costs, bistability occurs between a pathogen-free equilibrium and an endemic steady state (grey parameter region). The dashed red curve represents the minimum value of the force of infection scaling constant β where epidemics persist. See Table 1 for parameter values.

below 1.

When virulence increases mortality rates (Figure 2, middle panel), pathogen fitness, R_0, closely follows the increase in total population density, which is *mechanistically* governed by stage-specific competitive ability (the juvenile-adult ingestion asymmetry parameter, q). Epidemics are, therefore, more likely to occur in higher density, juvenile-dominated populations (high values of q, adults are competitively superior, development is resource-limited) relative to their adult-dominated counterparts (low values of q, juveniles are competitively superior, reproduction is resource-limited).

In contrast, when virulence increases maintenance costs (Figure 2, bottom panel), R_0 increases non-monotonically with changes in host population dynamics (and thus underlying changes in q). However, while the focus here is on infection-mediated increases in maintenance rates, this pattern is ultimately driven by differences in stage-specific mortality rates. When adults become strongly food-limited ($q \lesssim 0.676$, juveniles are competitively superior and reproduction is strongly resource-limited), infected adults starve and hence experience increased mortality. Infected juveniles, however, have

a positive net-energy production rate $\nu_J(\tilde{R})$, and mortality does not increase beyond the background rate. On the other hand, in environments where juveniles are strongly food-limited ($q \gtrsim 1.3$, adults are competitively superior and development is delayed), infected juveniles starve and mortality rates increase. Infected adults have a positive net-energy production rate $\nu_A(\tilde{R})$ and hence only experience background mortality. For cases where stage-specific competition is symmetric (intermediate values of q), infected juveniles and adults both starve and experience increased mortality. Pathogen fitness, R_0, reaches a maximum value at the transition from a regime with juveniles not starving to juveniles starving before increasing again for $q > 1$.

The relationships between the force of infection scaling constant, β, required for an outbreak to occur ($R_0 > 1$) and changes in host population demographics (governed by the juvenile-adult ingestion rate parameter, q) are largely similar to those for R_0 (Figure 3). When virulence increases mortality rates, the minimum value of β required for disease monotonically decreases with increasing values of q. That is, as populations shift from adult-dominated to juvenile-dominated. Mechanistically, this pattern emerges because the host population becomes increasingly dominated by juveniles, reproduction is no longer resource-limited, and total population density increases. In contrast, when virulence increases maintenance costs, the force of infection scaling constant, β, required for an outbreak to occur ($R_0 > 1$) reaches a local minimum $q \approx 0.676$. This point represents the transition between regimes with and without increased infection-mediated mortality for infected juveniles. For values of q above 1, the minimum value of the infection scaling parameter β that allows for pathogen invasion decreases again (Figure 3).

3.2. Equilibrium states with disease

The model shows pronounced variation in the effect of pathogens on host stability (Figures 4-6); depending on the initial stage structure of the susceptible host population that the pathogen invades and the specific form of virulence, pathogens can either destabilize or stabilize host populations. We will contrast model predictions for two different values of q: $q = 0.75$, in which case juvenile consumer-hosts are competitively superior and the population is consequently dominated by adult consumer-hosts, and $q = 1.25$, in which case adult consumer-hosts are competitively superior and the population is hence dominated by juvenile consumer-hosts.

Juvenile-dominated populations: adults competitively superior

When adults are competitively superior ($q = 1.25$), populations are dominated by juveniles, juvenile development is resource-limited, and total density is high (Figure 2). In this case the changes in the equilibrium state as a function of the force of infection (scaling parameter, β) resemble predictions from unstructured SI-models, irrespective of whether virulence increases mortality rates or maintenance costs (Figure 4). For values of β below the invasion threshold ($R_0 < 1$) the pathogen can not spread, while above this threshold increasing values of β shifts the population from susceptible to infected individuals. Since host demographics tend to be juvenile-dominated, the shift in density is more pronounced in juveniles relative to adults. When virulence increases maintenance costs, however, the change in the density of infected juveniles and adults is non-monotonic with the force of infection (scaling parameter, β). Surprisingly, the density of hosts decreases when infected individuals no longer

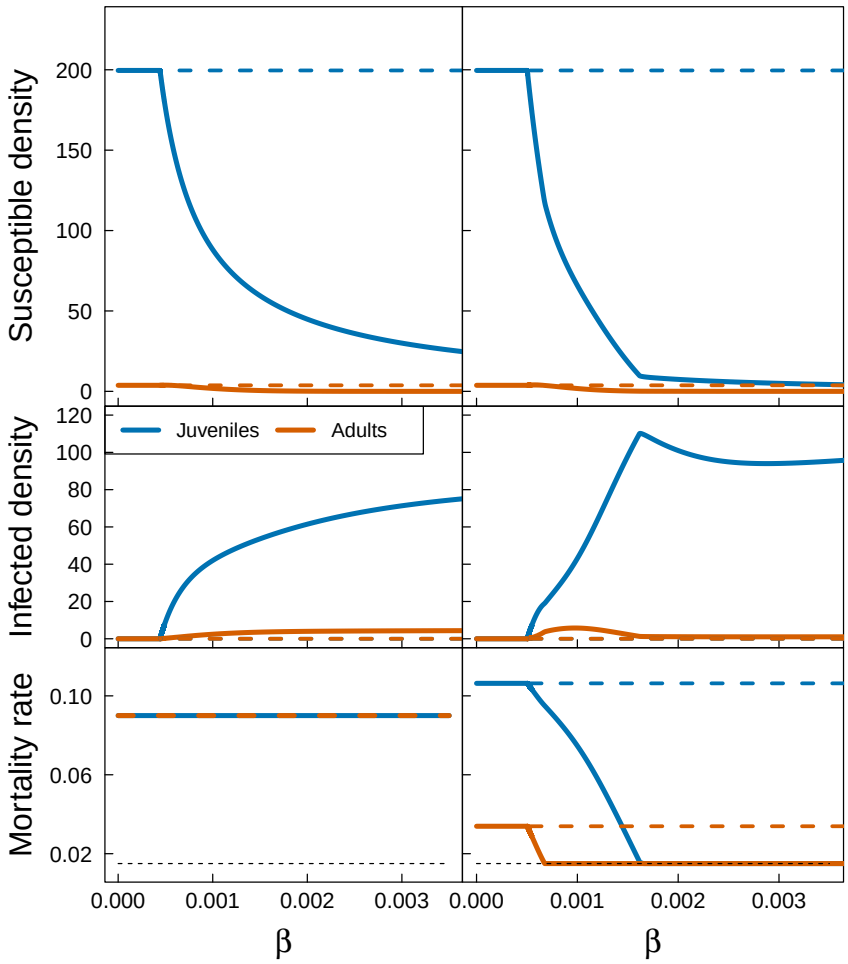

Figure 4. Equilibrium densities of susceptible (*top*) and infected (*middle*) juvenile (blue) and adult (orange) consumers-hosts in the endemic steady state with disease as a function of the force of infection (scaling constant, β). *Left column*: Virulence increases mortality rate (six times the mortality rate of susceptible individuals, $c_\mu = 5.0$). *Right Column*: Virulence increases (doubles) maintenance costs ($c_T = 1.0$). Bottom panels show the mortality rates of infected juvenile (blue) and adult (orange) hosts in the equilibrium state. Solid and dashed lines represent stable and unstable equilibrium states, respectively. Parameter values: $q = 1.25$ (juveniles are more food-limited), other parameters as in Table 1.

experience an increase in mortality (Figure 4, $\beta \gtrsim 0.0016$). Numerical integration studies of the dynamics also reveal that the equilibrium states are stable for $q = 1.25$, irrespective of the value of β and irrespective of whether or not the pathogen is present.

Adult-dominated populations, juveniles competitively superior

When juveniles are competitively superior ($q = 0.75$), populations are dominated by adults, reproduction is resource-limited, and total density is low (Figure 2). These changes in population structure lead to notably different patterns from those predicted by unstructured SI-models (Figure 5). When virulence increases mortality, the density of susceptible adults monotonically decreases with the force

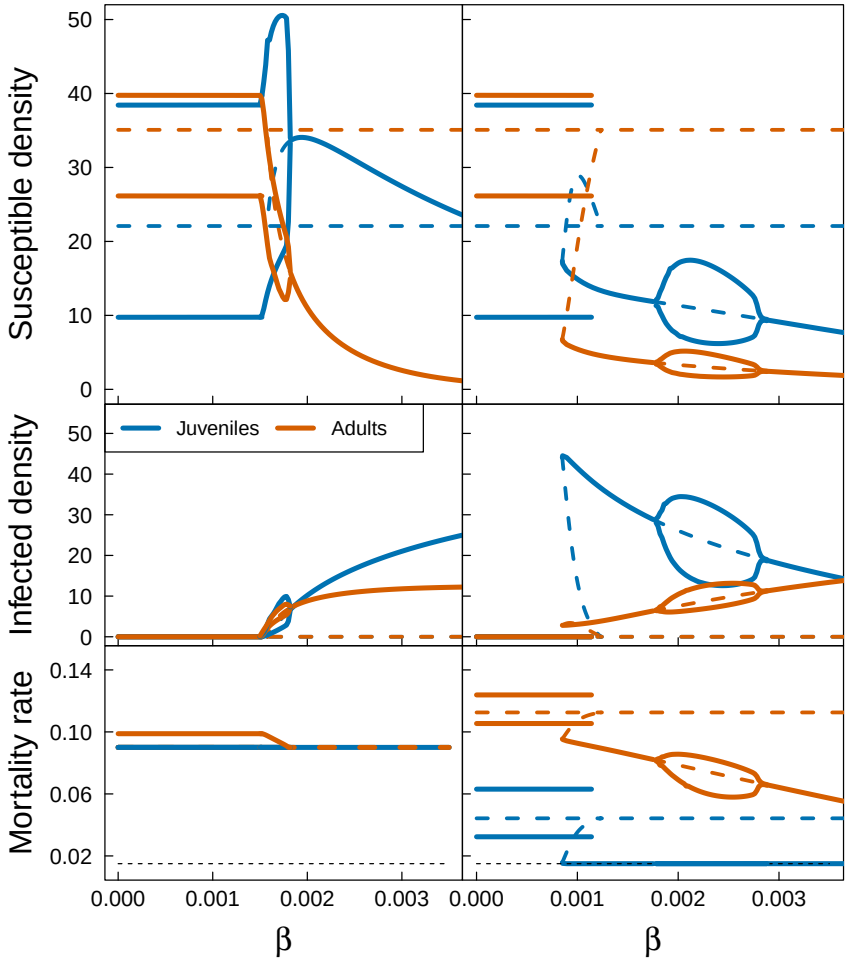

Figure 5. Equilibrium densities or maximum and minimum densities in case of oscillatory dynamics of susceptible (*top*) and infected (*middle*) juvenile (blue) and adult (orange) consumer-hosts in the endemic steady state with pathogens as a function of the force of infection (scaling constant, β). *Left column*: Virulence increases mortality rate (to six times the mortality rate of susceptible individuals, $c_\mu = 5.0$). *Right column*: Virulence increases (doubles) maintenance costs ($c_T = 1.0$). Bottom panels show the mortality rates for infected juvenile (blue) and adult (orange) hosts in the equilibrium state. Solid and dashed lines represent stable and unstable equilibrium states, respectively. Limit cycles occur at low values of β without pathogens and with pathogens for $\beta = 0.00152$ (threshold for pathogen invasion) to $\beta = 0.00182$ when virulence increases mortality rate (*left*) and for $\beta = 0.00178$ to $\beta = 0.00288$ when virulence increases maintenance costs (*right*). Maximum and minimum values occurring during the limit cycles are indicated with thick solid lines. Parameter values: $q = 0.75$ (juveniles are competitively superior, populations are dominated by adults, reproduction is more food-limited), other parameters as in Table 1.

of infection (scaling parameter, β) when pathogen establishment becomes possible, but the density of susceptible juveniles first increases with β before decreasing to values close to the density of juveniles in a fully susceptible population. In other words, pathogens mainly reduce the density of susceptible

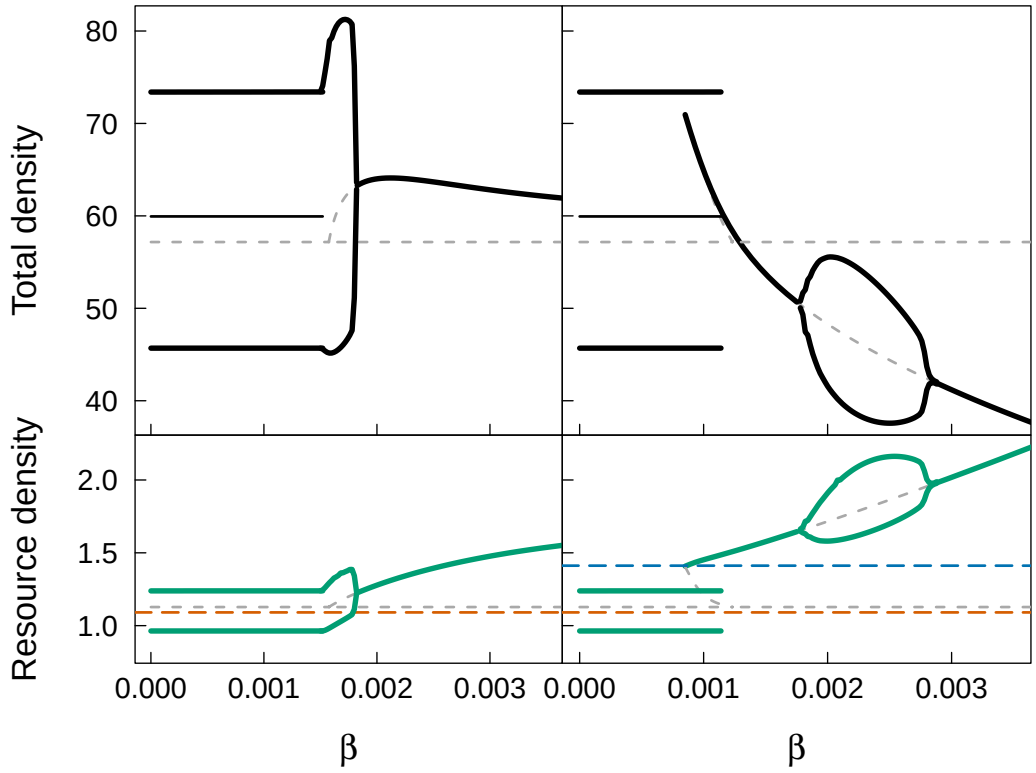

Figure 6. Same results as in Figure 5, but now showing total host density (*top*) and resource density (*bottom*) in the equilibrium state with and without pathogens as a function of the force of infection (scaling constant, β). *Left column*: Virulence increases mortality rate (to six times the mortality rate of susceptible individuals, $c_\mu = 5.0$). *Right column*: Virulence increases (doubles) maintenance costs ($c_T = 1.0$). Solid lines represent stable equilibrium states and maximum and minimum values occurring during limit cycles. Dashed lines represent unstable equilibrium states. The thin solid lines at low values of β in the top panels indicate the average total host density during the limit cycle of the susceptible-only population. The orange long-dashed horizontal lines in the bottom panel indicate the resource density, below which *susceptible adults* experience starvation mortality. The blue long-dashed horizontal lines in the right-bottom panel indicate the resource density, below which *infected juveniles* experience starvation mortality.

adults, not juveniles. The densities of infected juveniles and adults are always monotonically increasing with β.

Numerical integration studies of the dynamics reveal that for values of the force of infection (scaling parameter, β), that prevent pathogen invasion, the fully susceptible population exhibits stable limit cycles with much larger oscillations in juvenile densities. Once the pathogen can establish itself in the population, the amplitude of these population cycles first increases with β (Figure 5). However, further increases in β stabilize the dynamics, leading to a stable equilibrium state and juvenile-dominated populations. The pathogen therefore not only stabilizes the population cycles but does so by changing the population structure from adult-dominated to juvenile-dominated.

When virulence increases maintenance costs, the changes in equilibrium state as a function of the

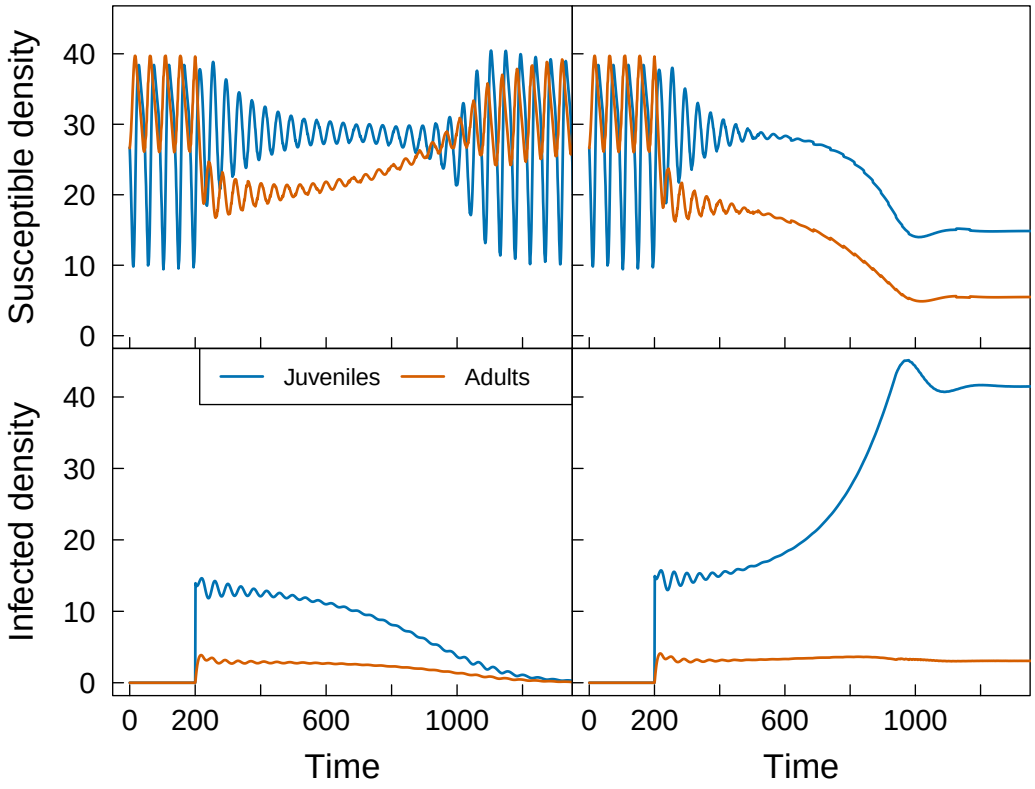

Figure 7. Dynamics of susceptible (*top*) and infected (*bottom*) densities of juveniles (blue) and adults (orange) when virulence increases (doubles) maintenance costs ($c_T = 1.0$), following the introduction of 14 (*left column*) or 15 (*right column*) infected newborn individuals into a fully susceptible population at time $t = 200$. Parameter values: $q = 0.75$ (adults are more food-limited), $\beta = 0.001$, other parameters as in Table 1.

force of infection (scaling parameter, β) are characterized by four prominent features: (*i*) as previously discussed, for low values of β that prevent pathogen invasion, the fully susceptible population exhibits stable limit cycles with much larger oscillations in juvenile densities; (*ii*) at the invasion threshold, where pathogen invasion becomes possible ($R_0 = 1$), a region of bistability occurs. In this region, stable limit cycles of the fully susceptible population emerge and co-occur alongside a stable equilibrium state with epidemics; (*iii*) pathogen establishment immediately stabilizes the limit cycle dynamics of the fully susceptible population, and (*iv*) for intermediate to large values of β ($0.00178 \lesssim \beta \lesssim 0.00288$) the equilibrium state with the pathogen becomes unstable and limit cycles occur with limited amplitude in all densities.

Figure 6 reveals that pathogens can increase the total population density of the host, irrespective of whether virulence increases mortality rate or maintenance costs. This hydra effect [41] occurs over a large range of β values when virulence increases host mortality. When virulence increases maintenance costs, the hydra effect only occurs in the bistable region, where stable limit cycles of the fully susceptible population co-occur alongside a stable equilibrium state with pathogens. Figure 6 also shows that, without pathogens, susceptible adults may starve and hence experience increased mortality during the limit cycle dynamics. Furthermore, when virulence increases maintenance costs, the endemic host-pathogen equilibrium state is feasible as long as infected juveniles do not experience

increased mortality due to starvation.

The bistable nature of the dynamics for values of β below the invasion threshold ($R_0 < 1$) is further illustrated in Figure 7. Before pathogen invasion (at time $t = 200$), the susceptible population exhibits oscillations with a period of approximately 50 time units. Introducing 14 or 15 infected newborn individuals into the population makes the difference between the pathogen going extinct or becoming established. Clearly, pathogens can not cause an epidemic from low host densities. Surprisingly, after pathogen establishment, the total density of juvenile individuals in the population is significantly higher than in the absence of pathogens. Even the total population density, including both susceptible and infected juveniles and adults is, on average, higher when the pathogen is endemic relative to the pathogen-free state.

4. Discussion and conclusions

We extended previously developed size-dependent theory [12] to test the hypothesis that pathogens should destabilize their host populations [42–45]. By explicitly linking infectious disease and the life history traits of juvenile and adult hosts that compete for shared resources, we developed the most mechanistic and comprehensive analysis of this hypothesis to date. Far from always destabilizing host populations, our results suggest that pathogens can have variable effects on the stability of host populations (Figures 4-6). Whether pathogens destabilized or stabilized host populations, depended on the initial stage structure of the host population and the specific form of virulence.

Pathogens stabilized host population cycles by shifting the population structure from adult-dominated to juvenile-dominated states. These results mirror empirical patterns observed in, for example, fungal-infected *Daphnia* [31] and trematode-infected snails [11]. Additionally, virulence that increased maintenance costs tended to stabilize host populations. These results, however, emerged because higher maintenance costs increased starvation mortality and therefore, host density, while simultaneously introducing a bottleneck in juvenile development and body size and/or adult fecundity. Mechanistically, these changes delayed when these individual-level effects were 'felt' at the population level.

Reductions in the density of consumer-hosts is a well-established stabilizing mechanism in both consumer-resource and epidemiological models [27,46,47]. Higher mortality for individual consumer-hosts increases stability because it reduces the maximum density of the hosts and thus, the intensity of grazing pressure on the resource. The resource, then, is less severely depressed and more limited (and stabilized) by density dependence. Thus, increased virulence prevents severe over-exploitation of the host's resource. This intriguing possibility suggests that pathogens may confer significantly underappreciated stability not only to their host populations but also to other species with which they interact. If pathogens stabilize their host populations, then removing pathogens from food webs could have unexpected and far-reaching consequences.

Our results also underscore that altering the stage structure of host populations could feedback to impact infectious diseases. In the model developed here, epidemics were larger when virulence increased maintenance costs, despite the reduction in host density, which should have reduced density-dependent transmission. Notably, these reductions in host density were small relative to those observed when virulence increased host mortality and therefore, an increase in the force of infection (faster transmission rates) was able to sustain pathogen outbreaks (Figure 5). Overall, juvenile-dominated

populations were subject to larger epidemics (Figure 1) and required a lower force of infection for pathogen invasion (Figure 2). Thus, our results also provide key insight into how the structure of host populations influences both the severity and trajectory of disease outbreaks (Figure 1).

The crucial links between the structure of host populations and infectious disease have long been recognized in epidemiology (unlike ecology, which has largely overlooked such interactions [14, 16]). For human pathogens, numerous data-guided mathematical models illustrate that accounting for host size, age, or stage often proves essential to understanding and managing outbreaks as seen, for example, with measles [20], pertussis [48], and rubella [49]. Biologically, accounting for differences in juvenile and adult hosts means that pathogens now face the additional challenge of exploiting a heterogeneous host population. This added complexity carries both epidemiological and evolutionary implications because a pathogen's fitness and ability to infect and spread through the population are determined by the frequency or density of each host type [22–24]. Yet, for the most part, existing studies on links between pathogens and stability have focused on homogeneous host populations. That is, all hosts are equally affected by infection and hold equal value for the pathogen.

This omission arises, in part, because layering in the impact of stage-specific effects on epidemiological dynamics into empirical or theoretical models is far from trivial. For example, stage-specific virulence (here, broadly defined as pathogen-induced harm) can arise through various mechanisms. As hosts grow and develop, the acquisition and allocation of energetic resources, encounter rates with parasites and pathogens, susceptibility to infection, and immune responses vary with age and body size [11, 31]. Additionally, for most species, body size is plastic, dependent on environmental conditions namely, resources that are required for maintenance, growth, and reproduction [12]. For infected hosts, resources also matter because responding to and coping with infection is energetically costly. The plastic and food-dependent nature of these traits govern host population structure, and may consequently influence epidemiological dynamics (Figure 1).

The surprising richness of dynamical outcomes generated by linking pathogens to the life history traits of juvenile and adult hosts is similar to those found in recent theoretical work, despite a number of notable differences between these two modeling frameworks [16]. To our knowledge, no existing models account for the resource dependence of these life history traits across multiple host stages in a continuous-time model. Other models for stage-specific epidemics include discrete-time models by Klepac and Caswell [50] who assume that population dynamics (demography) and infection happen sequentially instead of simultaneously. Additionally, Klepac and Caswell consider a host population that grows exponentially in the absence of pathogens. Whereas our model begins with a host population that is regulated by a resource and thus, density dependence even in the pathogen-free stage. More recent theoretical work by Simon *et al.* [16] examined cases where pathogens affect one stage or the other and infected juveniles mature into susceptible adults. Additionally, in their model, juvenile maturation depends on juveniles alone and does not include resource competition with adults. Such conditions primarily capture systems where stages do not overlap in location or have different diets. Under these conditions, virulence that delayed juvenile development or increased mortality tended to stabilize population dynamics. Similar to our model, Simon *et al.*, also found that an increase in mortality led to a counter-intuitive increase in population density, or hydra effect [13]. Together, each of these models helps identify various contexts where pathogens either stabilize or destabilize host populations.

The emergent properties uncovered with our model highlight that understanding the structuring

role of pathogens depends on resource availability, competitive interactions within and across host life stages, and different forms of virulence. For example, in juvenile-dominated populations, pathogen- and environmental-mediated feedbacks gave rise to complex dynamics including both biomass over-compensation [11, 12] and hydra effects [13, 41]. Identifying the essential mechanisms in our model that govern these emergent properties warrants deeper investigation and is the subject of ongoing work (Hite and de Roos *in progress*). Additionally, testing these predictions in empirical studies is an important future endeavor and an important step in improving our ability to predict and mitigate the effects of infectious diseases. In the meantime, these results underscore that considering these interactions can help propel studies working to understand how interventions targeting pathogens, specific host stages, forms of virulence may impact the other.

Use of AI tools declaration

The authors declare they have not used Artificial Intelligence (AI) tools in the creation of this article.

Code availability

The implementation of the Escalator Boxcar Train numerical method and the PSPM package used to analyze the model are located at https://github.com/amderoos/PSPM-disease.

Acknowledgments

We are grateful to three anonymous reviewers, Spencer Hall and Clay Cressler for insightful discussions that greatly improved this manuscript.

Conflict of interest

The authors declare there is no conflict of interest.

References

1. H. McCallum, A. Dobson, Detecting disease and parasite threats to endangered species and ecosystems, *Trends Ecol. Evolut.*, **10** (1995), 190–194. https://doi.org/10.1016/S0169-5347(00)89050-3
2. B. R. Forester, E. A. Beever, C. Darst, J. Szymanski, W. C. Funk, Linking evolutionary potential to extinction risk: applications and future directions, *Front. Ecol. Environ.*, **20** (2022), 507–515. https://doi.org/10.1002/fee.2552
3. J. Bosch, A. M.-C. de Alba, S. Marquínez, S. J. Price, B. Thumsová, J. Bielby, Long-term monitoring of amphibian populations of a National Park in northern Spain reveals negative persisting effects of Ranavirus, but not Batrachochytrium dendrobatidis, *Front. Veter. sci.*, **8** (2021). https://doi.org/10.3389/fvets.2021.645491
4. M. C. Fisher, T. W. Garner, Chytrid fungi and global amphibian declines, *Nat. Rev. Microbiol.*, **18** (2020), 332–343. https://doi.org/10.1038/s41579-020-0335-x

5. C. X. Cunningham, S. Comte, H. McCallum, D. G. Hamilton, R. Hamede, A. Storfer, et al., Quantifying 25 years of disease-caused declines in Tasmanian devil populations: host density drives spatial pathogen spread, *Ecol. Letters*, **24** (2021), 958–969. https://doi.org/10.1111/ele.13703
6. D. F. Jacobs, H. J. Dalgleish, C. D. Nelson, A conceptual framework for restoration of threatened plants: The effective model of American chestnut (Castanea dentata) reintroduction, *New Phytolog.*, **197** (2013), 378–393. https://doi.org/10.1111/nph.12020
7. F. De Castro, B. Bolker. Mechanisms of disease-induced extinction, *Ecol. Letters*, **8** (2005), 117–126. https://doi.org/10.1111/j.1461-0248.2004.00693.x
8. J. L. Hite, J. Bosch, S. Fernández-Beaskoetxea, D. Medina, S. R. Hall, Joint effects of habitat, zooplankton, host stage structure and diversity on amphibian chytrid, *Proceed. Royal Soc. B Biol. Sci.*, **283** (2016), 20160832. https://doi.org/10.1098/rspb.2016.0832
9. C. G. Becker, S. E. Greenspan, R. A. Martins, M. L. Lyra, P. Prist, J. P. Metzger, et al., Habitat split as a driver of disease in amphibians, *Biol. Rev.*, (2023). https://doi.org/10.1111/brv.12927
10. A. M. de Roos, J. A. J. Metz, L. Persson, Ontogenetic symmetry and asymmetry in energetics, *J. Math. Biol.*, **66** (2013), 889–914. https://doi.org/10.1007/s00285-012-0583-0
11. D. L. Preston, E. L. Sauer, Infection pathology and competition mediate host biomass overcompensation from disease, 2020. https://doi.org/10.1002/ecy.3000
12. A. M. de Roos, L. Persson. *Population and community ecology of ontogenetic development*, volume 51, Princeton University Press, 2013. https://doi.org/10.23943/princeton/9780691137575.001.0001
13. P. A. Abrams, When does greater mortality increase population size? The long history and diverse mechanisms underlying the hydra effect, *Ecol. letters*, **12** (2009), 462–474. https://doi.org/10.1111/j.1461-0248.2009.01282.x
14. A. M. de Roos, The impact of population structure on population and community dynamics, *Theor. Ecol.*, (2020), 53–73. https://doi.org/10.1093/oso/9780198824282.003.0005
15. R. Iritani, E. Visher, M. Boots, The evolution of stage-specific virulence: Differential selection of parasites in juveniles, *Evolut. Letters*, **3** (2019), 162–172. https://doi.org/10.1002/evl3.105
16. M. W. Simon, M. Barfield, R. D. Holt. When growing pains and sick days collide: Infectious disease can stabilize host population oscillations caused by stage structure, *Theoret. Ecol.*, **15** (2022), 285–309. https://doi.org/10.1007/s12080-022-00543-z
17. S. Panter, D. A. Jones, Age-related resistance to plant pathogens, *Adv. Botan. Res.*, **38** (2002), 251–280. https://doi.org/10.1016/S0065-2296(02)38032-7
18. B. Ashby, E. Bruns, The evolution of juvenile susceptibility to infectious disease, *Proceed. Royal Soc. B*, **285** (2018), 20180844. https://doi.org/10.1098/rspb.2018.0844
19. F. Ben-Ami, Host age effects in invertebrates: Epidemiological, ecological, and evolutionary implications, *Trends Parasitol.*, **35** (2019), 466–480. https://doi.org/10.1016/j.pt.2019.03.008
20. M. J. Keeling, P. Rohani, *Modeling Infectious Diseases in Humans and Animals*, Princeton University Press, 2008. https://doi.org/10.1515/9781400841035

21. S. Carran, M. Ferrari, T. Reluga, Unintended consequences and the paradox of control: Management of emerging pathogens with age-specific virulence, *PLoS Neglected Trop. Diseases*, **12** (2018), e0005997. https://doi.org/10.1371/journal.pntd.0005997

22. S. V. Cousineau, S. Alizon, Parasite evolution in response to sex-based host heterogeneity in resistance and tolerance, *J. Evolut. Biol.*, **27** (2014), 2753–2766. https://doi.org/10.1111/jeb.12541

23. F. Magpantay, A. King, P. Rohani, Age-structure and transient dynamics in epidemiological systems, *J. Royal Soc. Interface*, **16** (2019), 2019. https://doi.org/10.1098/rsif.2019.0151

24. A. Esteve, I. Permanyer, D. Boertien, J. W. Vaupel, National age and coresidence patterns shape COVID-19 vulnerability. *Proceed. Nat. Aca. Sci.*, **117** (2020), 16118–16120. https://doi.org/10.1073/pnas.2008764117

25. C. E. Cressler, D. V. McLeod, C. Rozins, J. Van Den Hoogen, T. Day, The adaptive evolution of virulence: a review of theoretical predictions and empirical tests, *Parasitology*, **143** (2016), 915–930. https://doi.org/10.1017/S003118201500092X

26. J. L. Abbate, S. Kada, S. Lion, Beyond mortality: Sterility as a neglected component of parasite virulence. *PLoS Pathogens*, **11** (2015), e1005229. https://doi.org/10.1371/journal.ppat.1005229

27. P. J. Hurtado, S. R. Hall, S. P. Ellner, Infectious disease in consumer populations: Dynamic consequences of resource-mediated transmission and infectiousness, *Theoret. Ecol.*, **7** (2014), 163–179. https://doi.org/10.1007/s12080-013-0208-2

28. V. H. Smith, R. D. Holt, M. S. Smith, Y. Niu, M. Barfield, Resources, mortality, and disease ecology: Importance of positive feedbacks between host growth rate and pathogen dynamics, *Israel J. Ecol. Evolut.*, **61** (2015), 37–49. https://doi.org/10.1080/15659801.2015.1035508

29. J. L. Hite, C. E. Cressler. Resource-driven changes to host population stability alter the evolution of virulence and transmission, *Philosophical Transactions of the Royal Society B: Biological Sciences*, **373** (2018), 20170087. https://doi.org/10.1098/rstb.2017.0087

30. C. J. Briggs, R. A. Knapp, V. T. Vredenburg, Enzootic and epizootic dynamics of the chytrid fungal pathogen of amphibians, *Proceed. Nat. Aca. Sci.*, **107** (2010), 9695–9700. https://doi.org/10.1073/pnas.0912886107

31. J. L. Hite, R. M. Penczykowski, M. S. Shocket, A. T. Strauss, P. A. Orlando, M. A. Duffy, et al., Parasites destabilize host populations by shifting stage-structured interactions, *Ecology*, **97** (2016), 439–449. https://doi.org/10.1890/15-1065.1

32. L. Persson, K. Leonardsson, A. M. de Roos, M. Gyllenberg, B. Christensen, Ontogenetic scaling of foraging rates and the dynamics of a size-structured consumer-resource model, *Theor. Popul. Biol.*, **54** (1998), 270–293. https://doi.org/10.1006/tpbi.1998.1380

33. K. Lika, R. M. Nisbet, A dynamic energy budget model based on partitioning of net production, *J. Math. Biol.*, **41** (2000), 361–386. https://doi.org/10.1007/s002850000049

34. A. M. de Roos, T. Schellekens, T. V. Kooten, K. E. V. D. Wolfshaar, D. Claessen, L. Persson, Simplifying a physiologically structured population model to a stage-structured biomass model, *Theor. Popul. Biol.*, **73** (2008), 47–62. https://doi.org/10.1016/j.tpb.2007.09.004

35. J. L. Hite, A. C. Pfenning, C. E. Cressler, Starving the enemy? Feeding behavior shapes host-parasite interactions, *Trends Ecol. Evolut.*, **35** (2020), 68–80. https://doi.org/10.1016/j.tree.2019.08.004
36. O. Diekmann, M. Gyllenberg, J. A. J. Metz, Steady-state analysis of structured population models, *Theor. Popul.n Biol.*, **63** (2003), 309–338. https://doi.org/10.1016/S0040-5809(02)00058-8
37. R. M. Anderson, R. M. May, *Infectious diseases of humans: Dynamics and control*, Oxford university press, 1992. https://doi.org/10.1093/oso/9780198545996.001.0001
38. J. Heesterbeek, K. Dietz, The concept of Ro in epidemic theory, *Statistica Neerlandica*, **50** (1996), 89–110. https://doi.org/10.1111/j.1467-9574.1996.tb01482.x
39. A. M. d. Roos, Numerical methods for structured population models: The Escalator Boxcar Train, *Numer. Methods Partial Differ. Equat.*, **4** (1988), 173–195. https://doi.org/10.1002/num.1690040303
40. A. M. d. Roos, O. Diekmann, J. A. J. Metz, Studying the dynamics of structured population models: A versatile technique and its application to Daphnia, *Am. Natural.*, **139** (1992), 123–147. https://doi.org/10.1086/285316
41. P. A. Abrams, H. Matsuda, The effect of adaptive change in the prey on the dynamics of an exploited predator population, *Canadian J. Fisher. Aquat. Sci.*, **62** (2005), 758–766. https://doi.org/10.1139/f05-051
42. R. M. Anderson, R. M. May, The invasion, persistence and spread of infectious diseases within animal and plant communities, *Philosoph. Transact. Royal Soc. London. B Biol. Sci.*, **314** (1986), 533–570. https://doi.org/10.1098/rstb.1986.0072
43. A. P. Dobson, The population biology of parasite-induced changes in host behavior, *Quarterly Rev. Biol.*, **63** (1988), 139–165. https://doi.org/10.1086/415837
44. Y. Xiao, F. Van Den Bosch, The dynamics of an eco-epidemic model with biological control, *Ecol. Model.*, **168** (2003), 203–214. https://doi.org/10.1016/S0304-3800(03)00197-2
45. A. Fenton, S. Rands, The impact of parasite manipulation and predator foraging behavior on predator–prey communities, *Ecology*, **87** (2006), 2832–2841. https://doi.org/10.1890/0012-9658(2006)87[2832:TIOPMA]2.0.CO;2
46. R. Anderson, R. M. May, Regulation and stability of host-parasite population interactions, *J. Animal Ecol.*, **47** (1978), 219–247. https://doi.org/10.2307/3933
47. F. M. Hilker, K. Schmitz, Disease-induced stabilization of predator–prey oscillations, *J. Theor. Biol.*, **255** (2008), 299–306. https://doi.org/10.1016/j.jtbi.2008.08.018
48. P. Rohani, X. Zhong, A. A. King, Contact network structure explains the changing epidemiology of pertussis, *Science*, **330** (2010), 982–985. https://doi.org/10.1126/science.1194134
49. C. J. E. Metcalf, J. Lessler, P. Klepac, A. Morice, B. T. Grenfell, O. Bjørnstad, Structured models of infectious disease: Inference with discrete data, *Theor. Popul. Biol.*, **82** (2012), 275–282. https://doi.org/10.1016/j.tpb.2011.12.001
50. P. Klepac, H. Caswell, The stage-structured epidemic: Linking disease and demography with a multi-state matrix approach model, *Theor. Ecol.*, **4** (2011), 301–319. https://doi.org/10.1007/s12080-010-0079-8

AIMS Press